



Correlation between optimized thicknesses of capping layer and thin metal electrode for efficient top-emitting blue organic light-emitting diodes

Hyunsu Cho  | Chul Woong Joo | Byoung-Hwa Kwon  | Chan-mo Kang | Sukyung Choi | Jin Wook Sin

ICT Creativity Research Laboratory,
Electronics and Telecommunications
Research Institute, Daejeon, Republic of
Korea

Correspondence

Hyunsu Cho, ICT Creativity Research
Laboratory, Electronics and
Telecommunications Research Institute,
Daejeon, Republic of Korea.
Email: hyunsucho@etri.re.kr

Funding information

Korea Evaluation Institute of Industrial
Technology (KEIT), Grant/Award
Numbers: 20012560 and 10079671.

Abstract

The optical properties of the materials composing organic light-emitting diodes (OLEDs) are considered when designing the optical structure of OLEDs. Optical design is related to the optical properties, such as the efficiency, emission spectra, and color coordinates of OLED devices because of the microcavity effect in top-emitting OLEDs. In this study, the properties of top-emitting blue OLEDs were optimized by adjusting the thicknesses of the thin metal layer and capping layer (CPL). Deep blue emission was achieved in an OLED structure with a second cavity length, even when the transmittance of the thin metal layer was high. The thin metal film thickness ranges applicable to OLEDs with a second microcavity structure are wide. Instead, the thickness of the thin metal layer determines the optimized thickness of the CPL for high efficiency. A thinner metal layer means that higher efficiency can be obtained in OLED devices with a second microcavity structure. In addition, OLEDs with a thinner metal layer showed less color change as a function of the viewing angle.

KEYWORDS

blue OLED, capping layer, microcavity, organic light-emitting diode, thin metal layer

1 | INTRODUCTION

Organic light-emitting diodes (OLEDs) with a top-emitting structure have been marketed and have become the standard for mobile displays. Both Samsung's Galaxy series and Apple's iPhone series have used OLED screens since the Galaxy S was released in 2010 and the iPhone X was released in 2017. OLED screens are increasingly being used in smartphones, tablets, and laptops that have lately been produced. Because it is self-emissive and has the advantages of a small and lightweight form factor,

top-emitting OLED has attracted attention recently, along with interest in augmented reality/virtual reality devices in the metaverse period [1]. Before the widespread production of OLED displays, intensive research on top-emitting OLED devices was conducted, and new technologies were developed in response to varied uses. One of the most essential technologies in top-emitting OLEDs is a top electrode comprised of a thin metal layer and a capping layer (CPL). Although indium tin oxide (ITO) is commonly used as a bottom electrode in bottom-emitting OLEDs, damage to organic layers makes the

sputtering deposition method and high-temperature annealing procedure incompatible with top electrodes in top-emitting OLEDs. Other transparent electrode materials, such as graphene, conductive polymers, metal nanowire, and others, have been used to improve the performance of organic optoelectronic devices [2–4]. Nevertheless, because of the manufacturing process, they are difficult to apply to the top electrodes. Thin metal layers, which can be deposited by thermal evaporation like organic molecules, have thus been considered potential top electrodes.

The optical and electrical properties of OLEDs are primarily determined by the thin metal layer. In terms of electrical efficiency, the lower the electrode's sheet resistance, the better. In terms of optical properties, the required characteristics of the electrode vary depending on the structure of the OLED device: High transmittance is required for white OLED devices, whereas monochromatic OLEDs require optimal transmittance capable of enhancing microcavity effects. Thin metal layers using various metals such as Ag, Au, and Cu were used as semitransparent electrodes. [5]. Among them, Ag has been widely used because of its low absorption and high conductivity. The formation of the thin metal layer is influenced by factors such as deposition temperature, deposition rate, and an underneath layer. To modify the metal growth dynamic of thin metal layers, various seed layers or wetting layers providing a good nucleation surface have been introduced [5]. For example, the codeposited small amount of Mg or Al improves conductivity and transmittance of the Ag thin metal layer [6]. Ultrathin metal layers with uniform and continuous morphologies can guarantee high conductivity and transmittance.

There is less restriction on the materials of CPL as CPL only plays an optical role. The transmittance of top electrodes can be controlled very effectively with just one layer [7–9]. Although organic and inorganic materials can be used as CPL, materials with a high refractive index are preferred because they can control the transmittance over a wide range. Until now, studies have mainly analyzed the optical properties of top-emitting OLED devices while maintaining the type and thickness of the thin metal layer and changing only the thickness of the CPL. A certain degree of reflectance of the top electrode is required to enhance the cavity effect in monochromatic OLEDs. Therefore, the thickness of the thin metal layer was applied to approximately 20 nm or more, and the reflectance was adjusted by controlling the thickness of the CPL. In this study, we change the both thickness of the thin metal layer and CPL to optimize the blue top-emitting OLEDs' efficiency and angular emission characteristics. In the blue OLED structure with a second cavity length, high color purity can be structurally

achieved even if the transmittance of the top electrode is high [10]. Mg-doped Ag with Mg:LiF seed layer was used as top electrodes. We reported that Mg:LiF/Mg:Ag electrodes formed uniform and continuous morphology from a 10-nm-thick and have high transmittance [6]. The relationship between their thicknesses and the emission properties of the top-emitting blue OLEDs was explored by raising the thickness of the thin metal layer from 10 nm and modifying the thickness of the CPL at the same time.

2 | EXPERIMENTS

2.1 | Optical simulation

For optical simulation, the commercial software SETFOS (Fluxim) was used. The refractive index (n) and extinction coefficient (k) of Mg-doped Ag are measured by spectroscopic ellipsometry (Figure S1). The n , k of organic materials and photoluminescence spectra of a blue fluorescent material were referred from the literature [11]. It is assumed that internal quantum efficiency is 100%, and an emission zone is placed in the center of an emission layer (EML). The blue OLED devices adopted the structure applied in the previous study [12]. The simulated OLED structure is Ag (100 nm)/hole transporting layer (HTL)/EML (20 nm)/electron transporting layer (ETL, 30 nm)/Mg:Ag/CPL as shown in Figure 1A. The simulated device structure was simplified compared to the fabricated device structure. The Mg:LiF layer was not considered because it is too thin. The refractive index of ITO and p-doped HTL were assumed to be similar to HTL. The HTL thicknesses were determined to fit the cavity length according to blue emission

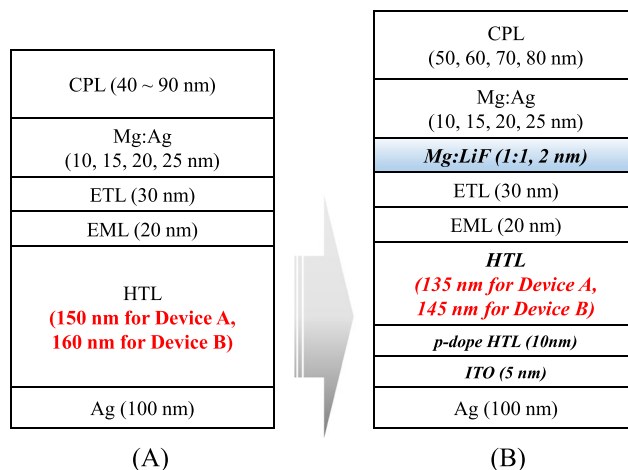


FIGURE 1 (A) OLED structure for optical simulation and (B) fabricated device structure

wavelength. For the two device structures having HTL thicknesses of 150 nm (Device A) and 160 nm (Device B), optical properties were simulated according to the thickness of Mg:Ag and CPL.

2.2 | Thin metal and OLED device fabrication

Thin metal layers and OLED devices were fabricated on bare glass substrates and ITO (5 nm)/Ag (100 nm)/ITO (5 nm) prepatterned glass substrates, respectively. The substrates were sequentially cleaned in an ultrasonication bath with acetone, isopropyl alcohol, and deionized water and then dried in an 80°C vacuum oven. The substrates are then transferred to a thermal evaporation chamber to deposit organic materials and metals. Thin metal layers (neat Ag and Mg:Ag [1:10]) were deposited on Mg:LiF (1:1, 2 nm)/ETL (30 nm) to measure the optical and electrical properties of thin metal layers. Figure 1B shows the structure of the fabricated OLED device, which differs slightly from the OLED device structure used in the simulation: p-doped HTL (10 nm) was deposited to improve electrical properties, and the HTL was deposited by the thickness obtained from the simulation excluding the ITO thicknesses and p-doped HTL. Additionally, Mg:LiF (1:1, 2 nm), which was omitted in the simulation, was deposited between the ETL and the Mg:Ag electrodes to improve electron injection. The fabricated OLED devices were encapsulated using ultraviolet (UV) light curing epoxy resins (Nagase ChemteX Corporation) in an N_2 -filled glove box.

2.3 | Thin metal and OLED device characterization

A UV/Vis/NIR spectrophotometer (Perkin Elmer, Lambda 950) and a four-point probe (AIT, MT-SR2000N) were used to test the transmittance and sheet resistance of thin metal layers. A source meter (Keithley 238) and a spectroradiometer (Minolta, CS-2000) were used to measure the current density(J)–voltage(V)–luminance(L) and electroluminescence (EL) spectra of OLED devices.

3 | RESULTS AND DISCUSSION

3.1 | Thin metal characteristics

Figure 2 shows the transmittance of Mg:Ag and neat Ag thin films for their thicknesses. The critical thickness is the thickness at which metal islands begin to form

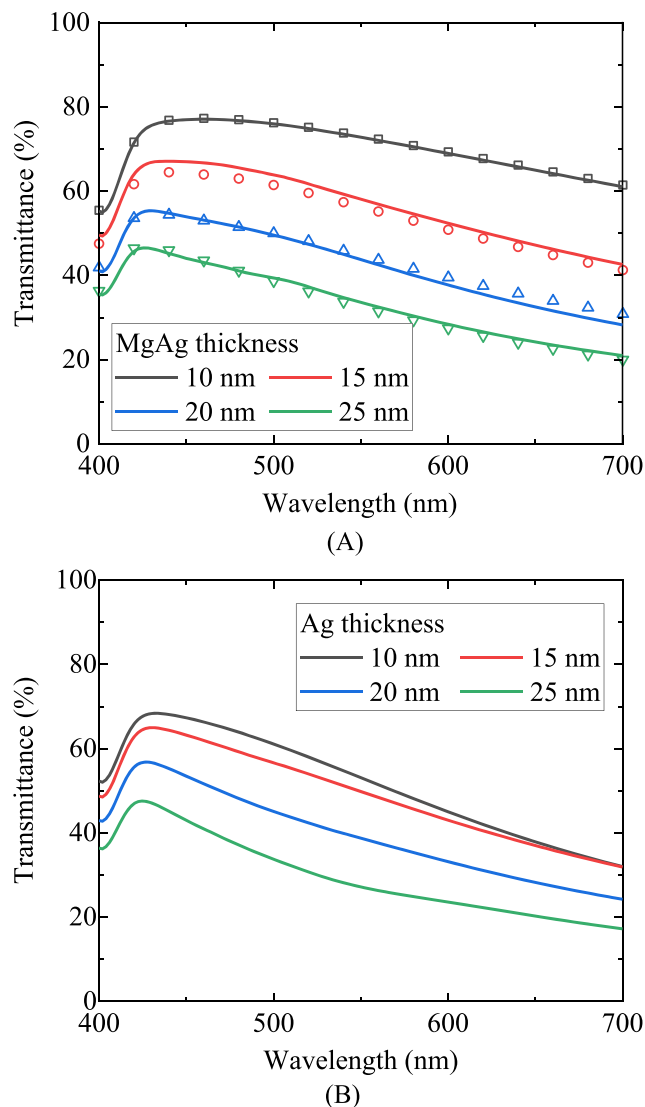


FIGURE 2 Transmittance of (A) Mg:Ag and (B) neat Ag on Mg:LiF/ETL for thickness 10, 15, 20, and 25 nm. The dots shown in (A) are simulated transmittance

continuous films, and that of Mg:Ag thin film is 8 nm–10 nm [6]. Further increasing the thin metal thickness above the critical thickness, its transmittance decreases, which is attributed to the increase in reflectivity of the thin metal layer [13, 14]. Consequently, the Mg:Ag thin film transmittance decreases in proportion to the thickness. However, the neat Ag thin films have similar transmittance at 10 nm and 15 nm, and their transmittance decreases like the Mg:Ag thin film at a thickness above 15 nm. The neat Ag thin film has discontinuous morphology at 10 nm and a critical thickness between 10 nm and 15 nm.

Table 1 shows the sheet resistance of Mg:Ag and neat Ag thin film for their thicknesses. At the thickness of 10 nm, the Mg:Ag sheet resistance is smaller than that of the neat Ag thin film. This result is consistent with the

TABLE 1 Sheet resistance ($\Omega/\text{sq.}$) of Mg:Ag and neat Ag

Thickness (nm)	10	15	20	25
Mg:Ag	13.4	9.3	6.7	3.8
Ag	60.4	6.8	3.2	2.1

transmittance result because the Mg:Ag thin film with a thickness thicker than the critical thickness has a more uniform and continuous morphology than the Ag thin film with a thickness thinner than the critical thickness. When both thin films have a thickness thicker than the critical thickness, the sheet resistance of the Ag thin film is smaller than that of the Mg:Ag thin film because Ag has higher conductivity than Mg [15].

3.2 | Optical simulation

The Mg:Ag thin film can adjust transmittance more extensively than the neat Ag thin film through thickness control. If the Mg:Ag thin film with a CPL capable of tuning transmittance is used as the top electrode, various optical properties of top-emitting OLED devices can be obtained. Before simulating the OLED device's optical properties according to the thickness of the Mg:Ag thin film and the CPL, the n, k of the Mg:Ag thin film was verified. Generally, a n, k of a thin metal film varies depending on the thickness or process conditions. The n, k of the Mg:Ag thin film used in this study shown in Figure S1 has an intermediate value of the n, k according to the thickness of the neat Ag thin film published in a previous paper [16]. A single n, k value was applied to the Mg:Ag thin film regardless of its thicknesses because the thickness above 10 nm was thicker than the critical thickness [6]. Consequently, it was confirmed that the simulated transmittance was almost similar to the measured value by adjusting only the thickness, as shown in Figure 2A.

Based on this n, k value, the optical properties of the top-emitting OLEDs were simulated according to the HTL thickness: HTL thicknesses are 135 and 145 nm for devices A and B, respectively. Figure 3A,B shows the Luminance and Commission Internationale de l'éclairage (CIE) y-color coordinate (CIEy) of devices A and B for the thicknesses of Mg:Ag and CPL. When evaluating blue OLEDs, these two factors are crucial [17]. The smaller CIEy is preferred for a high color gamut. However, as the CIEy becomes smaller, the overlap with the photopic response curve decreases, which is rather a disadvantage in terms of Luminance. Hence, it is important to compromise these two characteristics properly.

Regardless of the thicknesses of Mg:Ag and CPL, Device A has less Luminance and smaller CIEy than

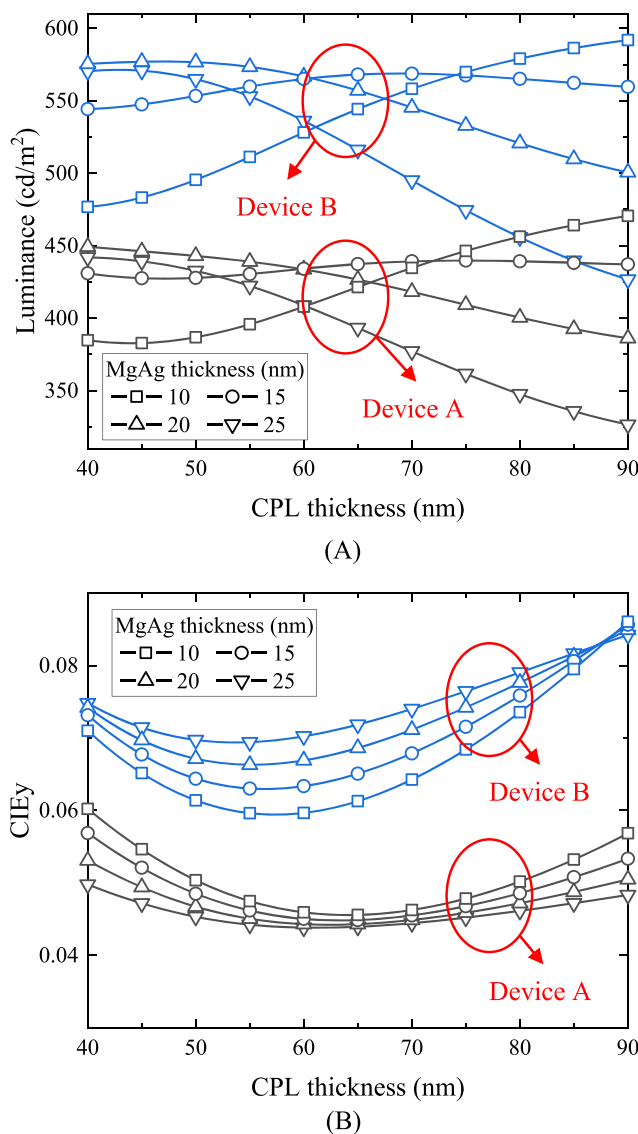


FIGURE 3 (A) Luminance and (B) Commission Internationale de l'éclairage (CIE) y-color coordinate (CIEy) of devices A and B for the thicknesses of Mg:Ag and capping layer (CPL)

Device B because the HTL thickness of Device A is thinner than that of Device B. As the HTL thickness decreases, the cavity length decreases; thus, the cavity resonant wavelength of the OLED device is blueshifted. The Luminance varies considerably depending on the thicknesses of Mg:Ag and CPL, and the tendency is similar in devices A and B, as shown in Figure 3A. Depending on the thickness of the CPL, the luminance change in a device with 15-nm-thick Mg:Ag is minimal. However, a device with 10-nm-thick Mg:Ag increases Luminance as the CPL thickness increases. If the thickness of the CPL is increased further, the Luminance has a maximum

value at approximately 100 nm and decreases again when the thickness of the CPL is greater than that shown in Figure S2. This is because the transmittance of Mg:Ag with CPL increases and decreases as the thickness of the CPL increases [7–9]. Conversely, a device with 20- and 25-nm-thick Mg:Ag has a high luminance when the thickness of the CPL is thin. Therefore, the CPL thickness should be optimized according to the thickness of the thin metal film.

In both devices, the CIEy is less than 0.08 in all thicknesses of Mg:Ag and CPL used in the simulation, and the requirement for blue emission based on the NTSC standard was satisfied. However, because of the recently required high color gamut, only Device A can attain CIEy of less than 0.046 based on BT.2020 standard. Even if the thickness of the thin metal film becomes thin and its transmittance is increased, sufficient blue color coordinates may be ensured as long as the cavity length is well matched in a device with a second cavity structure. Unlike Luminance, the CIEy has a smaller change according to the thickness of the CPL as the thickness of Mg:Ag increases. Furthermore, when the thickness of Mg:Ag is thin, the CIEy in Device B are small, whereas in Device A, the CIEys are small when Mg:Ag is thick.

3.3 | Blue OLED device characteristics

Figure S3 shows the J–V and L–V characteristics of Devices A and B according to Mg:Ag and CPL thicknesses. Regardless of both thicknesses, J–V characteristics are similar. The Mg:Ag with a thickness of 10 nm or more has a sufficiently low sheet resistance, as shown in Table 1, and electron injection from the Mg:Ag electrode to the ETL is effective [6]. Therefore, the thickness of Mg:Ag has no effect on electrical properties. Furthermore, because CPL is located above the electrode in top-emitting OLEDs, it is not included in the device's active layer and does not influence electrical properties. There is a slight difference in J between devices A and B, which is caused by the difference in HTL thickness. In Device B, where HTL is thicker, the electric field is relatively small at the same V, so the J is a little lower.

Unlike electrical properties, optical properties are significantly influenced by the thicknesses of Mg:Ag and CPL. The transmittance of the top electrode in OLEDs varies substantially according to the thickness of Mg:Ag as shown in Figure 2A, as well as to the thickness of CPL. Figure 4A shows the current efficiency (CE) of devices A and B for the Mg:Ag and CPL thickness. Among external quantum efficiency, CE, and power efficiency, which are various variables that express the efficiency of OLED, CE is mainly used to evaluate an

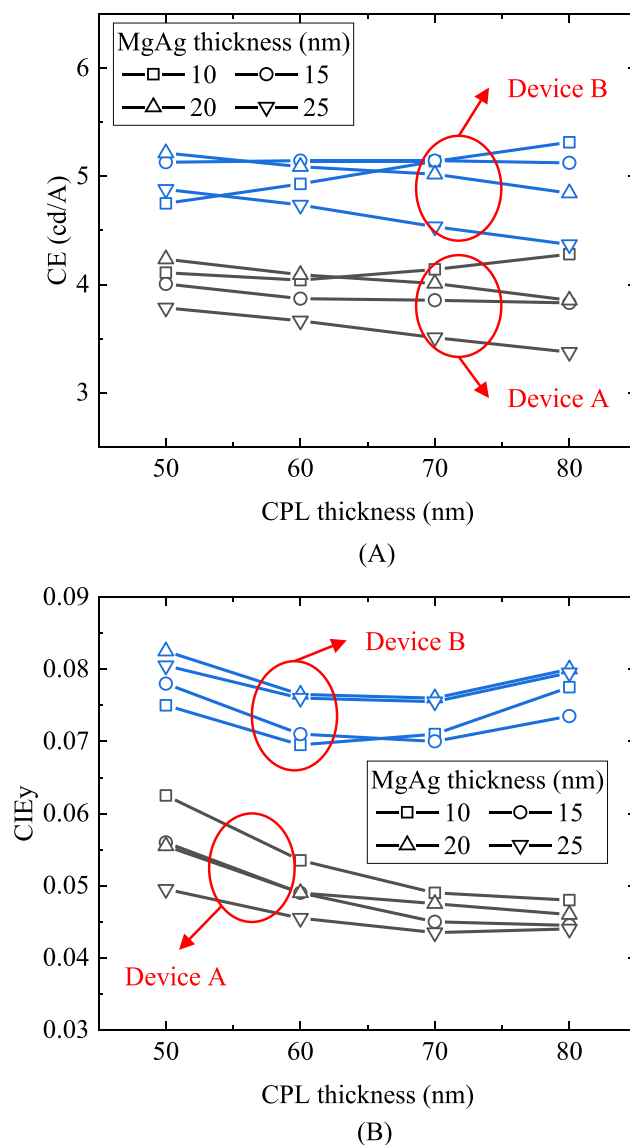


FIGURE 4 (A) Current efficiency and (B) Commission Internationale de l'éclairage (CIE) y-color coordinate of Device A and Device B for the thicknesses of Mg:Ag and capping layer (CPL)

efficiency of top-emitting OLEDs. Experimental results show a similar tendency compared with the simulation results, as shown in Figure 3A. As mentioned previously, the thickness of Mg:Ag and CPL has no effect on electrical properties; hence, the change in L is proportional to the change in CE. The tendency of CE changes depending on the thickness of Mg:Ag and CPL is similar in devices A and B. Because the HTL thickness is thicker and the resonant wavelength is closer to 550 nm, the CEs of Device B are higher than those of Device A.

The CE of OLEDs with 10-nm-thick Mg:Ag increases as the thickness of the CPL increases. Conversely, the CE of OLEDs with 25-nm-thick Mg:Ag decreases as the thickness of the CPL increases. In OLEDs with 15- and

20-nm-thick Mg:Ag, CE changes relatively less sensitively to the CPL thickness. The highest CE can be obtained in both devices A and B when Mg:Ag thickness is thin (10 nm) and CPL thickness is thick (80 nm). The transmittance and reflectance of the top electrode at the emission wavelength of blue OLEDs (460 nm) changed according to the thickness of Mg:Ag and CPL, as shown in Figure S4. Reflections occur at the ETL/Mg:Ag, the Mg:Ag/CPL, and the CPL/Air interfaces. The interference between them is influenced by the thickness of the Mg:Ag layer and CPL [18]. Considering the relatively broad PL spectrum of the blue dopant and a second cavity structure, the efficiency can deteriorate if the transmittance is too low (the reflectivity is too high) and the microcavity effect is too strong. This contradicts the result that the thickness of Ag in a blue OLED with a first cavity structure must be thick to increase efficiency and color purity [19].

Figure 4B shows the CIEy of Devices A and B for the Mg:Ag and CPL thicknesses. These experimental results also show a similar tendency to the simulation results. Because of a thicker HTL in Device B than in Device A, the CIEy of Device B is higher than that of Device A. CIEy is dominantly affected by Mg:Ag thickness than by CPL thickness. In Device A, when the Mg:Ag thickness is thin, the CIEys are large. Conversely, in Device B, when the Mg:Ag thickness is thick, the CIEy is large. It is necessary to confirm the spectra changes depending on the thickness of Mg:Ag and CPL to analyze the change in CE and CIEy. Figure 5A,B shows the normalized electroluminescent (EL) spectra according to the thickness of the Mg:Ag and CPL in device A and B, respectively. As the thickness of the Mg:Ag increases, its reflectance increases, and its transmittance decreases. As shown in (1), the reflectance and transmittance of the top electrode is strongly related to the Fabry-Pérot (f_{FP}) factor, which influences the microcavity effect [11].

$$f_{FP} = \frac{T_{top}}{(1 - \sqrt{R_{top}R_{bot}})^2 + 4\sqrt{R_{top}R_{bot}}\sin^2\left(\frac{\Delta\phi}{2}\right)}, \quad (1)$$

where T_{top} and R_{top} are the transmittance and the reflectance through the Mg:Ag electrode from the organic layer, respectively. R_{bot} are the reflectance at organic/bottom electrode interfaces, and $\Delta\phi$ is the phase change term. The f_{FP} increases as the reflectance increases and the transmittance decreases. Therefore, the microcavity effect is enhanced, and the full width at half maximum (FWHM) of the EL spectra decreases preferentially as the Mg:Ag thickness increases. Depending on the CPL thickness, the FWHM of the EL spectra can change slightly more. As the CPL thickness increases, the transmittance of the top electrode decreases, as shown in Figure S4. As

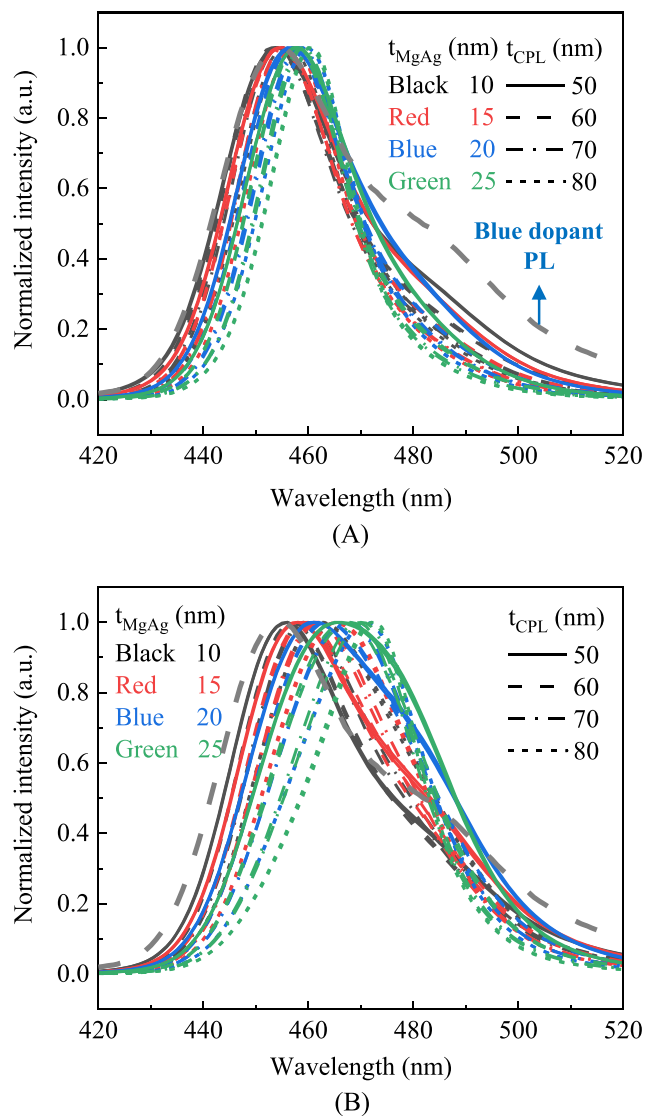


FIGURE 5 Normalized electroluminescent spectra of (A) Device A and (B) Device B depending on the thickness of Mg:Ag and capping layer (CPL)

a result, emission at a wavelength of 480 nm or more decreases, and the CIEy decreases in Device A.

The peak of EL spectra is shifted to a longer wavelength as the Mg:Ag thickness increases in Device B. The increased thickness of the HTL shifts the cavity resonant wavelength to the long wavelength in blue photoluminescent (PL) emission. The emission near the shoulder emission peak wavelength region (465 nm–470 nm) of the blue dopant is enhanced when the Mg:Ag thickness increases and the microcavity effect increases. Therefore, as the Mg:Ag thickness increases, the CIEy increases.

Blue OLEDs with a second cavity structure can obtain sufficiently low CIEy even if the Mg:Ag thickness is thin.

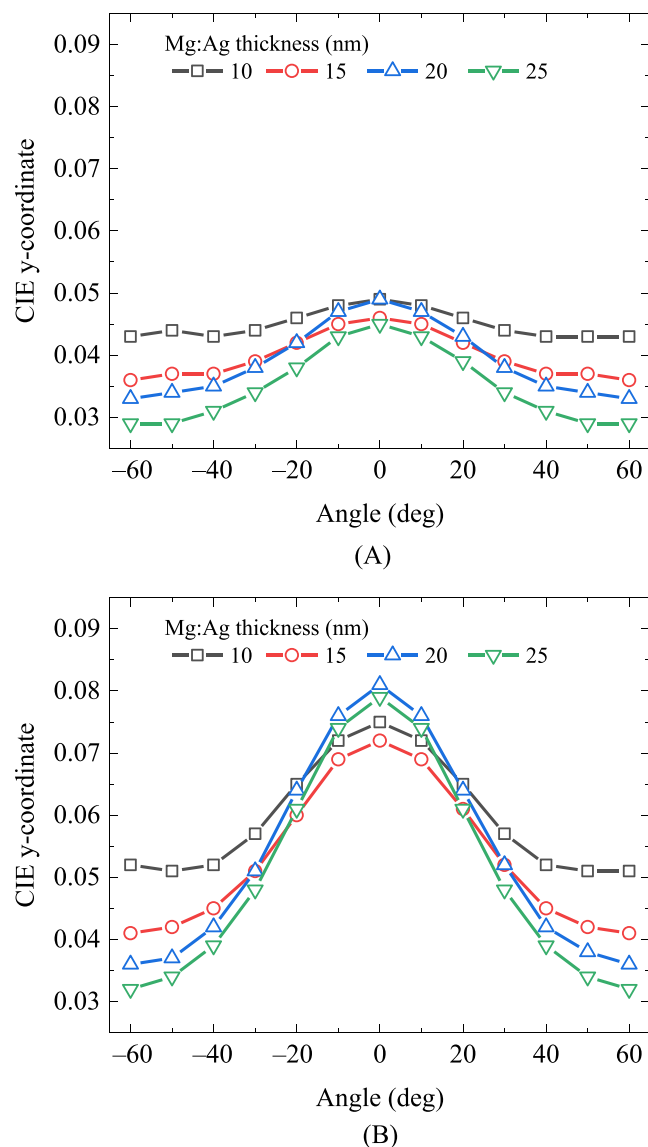


FIGURE 6 Commission Internationale de l'éclairage (CIE) y-color coordinate change according to the viewing angle of (A) Device A and (B) Device B with 70-nm-thick capping layer (CPL) depending on the thickness of Mg:Ag

Rather, if the CPL thickness is optimized, the lower the Mg:Ag thickness, the higher the efficiency may be obtained. Another advantage of OLEDs with a thin Mg:Ag thickness is that the spectral change according to the viewing angle is small. Figure 6A,B shows CIEy change according to the viewing angle of Devices A and B with 70-nm-thick CPL, respectively. As the viewing angle increases, the cavity resonant wavelength is blueshifted, and the CIEy in blue OLEDs becomes smaller [20]. In all devices, the CIEy decreases as the viewing angle increases. The change in CIEy is larger for OLED devices

with thicker metal thin films. In both structures, OLEDs with 10-nm-thick Mg:Ag exhibit smaller CIEy changes with the viewing angle than OLEDs with different Mg:Ag thicknesses. The thicker the metal thin film, the stronger the microcavity effect, which aggravates such a phenomenon. The strong microcavity effect can increase the color purity of the emission spectrum. However, the shape of the emission spectrum changes considerably when the cavity peak changes according to the viewing angle. Therefore, the color change is small in the OLEDs with thin Mg:Ag.

When the two device structures are compared, Device A has a smaller CIEy change according to the viewing angle than Device B. Because Device A has a thinner HTL than Device B, the cavity resonant wavelength of Device A is matched to the shorter wavelength in blue PL emission at a viewing angle of 0°. The shift in the cavity resonant wavelength increasingly deviates from the blue PL emission as the viewing angle increases. Therefore, the CIEy does not change significantly even if the viewing angle increases. Instead, as shown in Figure S5, the decrease in luminance according to the viewing angle is more severe.

4 | CONCLUSIONS


In this study, we investigated the optimized thicknesses of a thin metal layer and CPL in top-emitting blue OLEDs with a second cavity structure. The CPL thickness to which efficiency and CIEy are optimized varies according to the Mg:Ag electrode thickness. When the thickness of Mg:Ag is thin, the thicker the CPL, the more optimized the efficiency and CIEy are. Conversely, when the thickness of Mg:Ag is thick, the thinner the CPL is, the more optimized they are. Consequently, unlike the first cavity structure, in the second cavity structure, higher efficiency can be obtained when the thickness of the thin metal film is thin. The Mg:Ag thin film shows low sheet resistance even at 10 nm, and it was applied as a top electrode with 80-nm-thick CPL to achieve a CE of 5.3 cd/A. Furthermore, the color coordinate change was confirmed to be small as the thickness of the thin metal film was thinner.

CONFLICT OF INTEREST

The authors declare that there are no conflicts of interest.

ORCID

Hyunsu Cho  <https://orcid.org/0000-0003-0182-6376>

Byoung-Hwa Kwon  <https://orcid.org/0000-0002-5435-6323>

REFERENCES

1. C. Kang and H. Lee, *Recent progress of organic light-emitting diode microdisplays for augmented reality/virtual reality applications*, J. Inf. Disp. **23** (2022), 19–32.
2. D. S. Hecht, L. Hu, and G. Irvin, *Emerging transparent electrodes based on thin films of carbon nanotubes, graphene, and metallic nanostructures*, Adv. Mater. **23** (2011), 1482–1513.
3. W. Cao, J. Li, H. Chen, and J. Xue, *Transparent electrodes for organic optoelectronic devices: a review*, J. Photon. Energy **4** (2014), 040990.
4. M. Morales-Masis, S. D. Wolf, R. Woods-Robinson, J. W. Ager, and C. Ballif, *Transparent electrodes for efficient optoelectronics*, Adv. Electron. Mater. **3** (2017), 1600529.
5. Y. -G. Bi, Y. -F. Liu, X. -L. Zhang, D. Yin, W. -Q. Wang, J. Feng, and H. -B. Sun, *Ultrathin metal films as the transparent electrode in ITO-free organic optoelectronic devices*, Adv. Opt. Mater. **7** (2019), 1800778.
6. H. Cho, C. W. Joo, S. Choi, C. M. Kang, B. H. Kwon, J. W. Shin, K. Kim, D. H. Ahn, N. S. Cho, and G. H. Kim, *Highly conductive and transparent thin metal layer for reducing micro-cavity effect in top-emitting white organic light-emitting diode*, Org. Electron. **106** (2022), 106537.
7. H. Riel, S. Karg, T. Beierlein, B. Ruhstaller, and W. Rieß, *Phosphorescent top-emitting organic light-emitting devices with improved light outcoupling*, Appl. Phys. Lett. **82** (2003), 466–468.
8. C. -C. Wu, C. -L. Lin, P. -Y. Hsieh, and H. -H. Chiang, *Methodology for optimizing viewing characteristics of top-emitting organic light-emitting devices*, Appl. Phys. Lett. **84** (2004), 3966–3968.
9. Q. Huang, K. Walzer, M. Pfeiffer, K. Leo, M. Hofmann, and T. Stübinger, *Performance improvement of top-emitting organic light-emitting diodes by an organic capping layer: an experimental study*, J. Appl. Phys. **100** (2006), 064507.
10. S. Hofmann, M. Thomschke, P. Freitag, M. Furno, B. Lüssem, and K. Leo, *Top-emitting organic light-emitting diodes: influence of cavity design*, Appl. Phys. Lett. **97** (2010), 253308.
11. H. Cho, C. W. Joo, S. Choi, C. M. Kang, G. H. Kim, J. W. Shin, B. H. Kwon, H. Lee, C. W. Byun, and N. S. Cho, *Design of white tandem organic light-emitting diodes for full-color microdisplay with high current efficiency and high color gamut*, ETRI j. **43** (2021), 1093–1102.
12. J. Park, J. -H. Lee, J. Lee, and H. Cho, *Effect of a p-doped hole transport and charge generation layer on single and two-tandem blue top-emitting organic light-emitting diodes*, J. Inf. Disp. **22** (2021), 107–113.
13. M. Wu, S. Yu, L. He, L. Yang, and W. Zhang, *High quality transparent conductive Ag-based barium stannate multilayer flexible thin films*, Sci. Rep. **7** (2017), 103.
14. L. Peres, A. Bou, D. Barakel, and P. Torchio, *ZnS[ag]TiO₂ multilayer electrodes with broadband transparency for thin film solar cells*, RSC Adv. **6** (2016), 61057–61063.
15. S. -K. Kwon, E. -H. Lee, K. -S. Kim, H. -C. Choi, M. J. Park, S. K. Kim, R. Pode, and J. H. Kwon, *Efficient micro-cavity top emission OLED with optimized Mg:Ag ratio cathode*, Opt. Express **25** (2017), 29906–29915.
16. X. Liu, X. Cai, J. Qiao, J. Mao, and N. Jiang, *The design of ZnS/Ag/ZnS transparent conductive multilayer films*, Thin Solid Films **441** (2003), 200–206.
17. J. -H. Lee, C. -H. Chen, P. -H. Lee, H. -Y. Lin, M. K. Leung, T. L. Chiu, and C. F. Lin, *Blue organic light-emitting diodes: current status, challenges, and future outlook*, J. Mater. Chem. C **7** (2019), 5874–5888.
18. C. Ji, D. Liu, C. Zhang, and L. Jay Guo, *Ultrathin-metal-film-based transparent electrodes with relative transmittance surpassing 100%*, Nat. Commun. **11** (2020), 3367.
19. W. Ren, K. R. Son, T. H. Park, V. Murugadoss, and T. G. Kim, *Manipulation of blue TADF top-emission OLEDs by the first-order optical cavity design: toward a highly pure blue emission and balanced charge transport*, Photon Res **9** (2021), no. 8, 1502–1512.
20. E. Kim, J. Chung, J. Lee, H. Cho, N. S. Cho, and S. Yoo, *A systematic approach to reducing angular color shift in cavity-based organic light-emitting diodes*, Org. Electron. **48** (2017), 348–356.

AUTHOR BIOGRAPHIES



Hyunsu Cho received his BS and PhD degrees in electrical engineering from the Korea Advanced Institute of Science and Technology, Daejeon, Republic of Korea in 2008 and 2014, respectively. He joined the Electronics and Telecommunications Research Institute, Daejeon, Republic of Korea, in 2014 and is currently a Senior Researcher. His research interests include the device physics and optical design of optoelectronics devices, such as organic light-emitting diodes (OLEDs).



Chul Woong Joo received his BS and MS degrees in polymer science and engineering of organic electronics devices from Dankook University, Yongin, Republic of Korea in 2008 and 2010, respectively. He is currently a senior researcher at the Electronics and Telecommunications Research Institute (ETRI), Daejeon, Republic of Korea. His current research interests include flexible display devices and microdisplays for augmented reality/virtual reality applications.



Byoung-Hwa Kwon received his BS, MS, and PhD degrees from the Department of Materials Science & Engineering of Hanyang University, Pohang University of Science and Technology, and Korea Advanced Institute of Science and Technology, Republic of Korea, respectively, in 2006, 2008, and 2012. After graduating, he worked in the Department of Materials Science & Engineering of the University of Florida in Gainesville, USA as a postdoctoral

associate and at LG Chem Ltd as a senior researcher. He joined the Electronics and Telecommunications Research Institute, Daejeon, Republic of Korea, in 2014. His current research interests are optoelectronic materials and devices, such as OLEDs, QD (quantum dot)-LEDs, photodetectors, and thin-film encapsulation for flexible devices.



Chan-mo Kang received his BS and PhD electrical and computer engineering degrees from Seoul National University, Seoul, Republic of Korea in 2008 and 2014, respectively. He is currently a senior researcher at the Electronics and Telecommunications

Research Institute, Daejeon, Republic of Korea. His research interests include device engineering and physics in organic electronics, thin-film transistors, organic/inorganic hybrid devices, and high-resolution displays for augmented reality/virtual reality applications.



Sukyung Choi received her BS degree at the Department of Nanomaterials Engineering from Pusan National University, Pusan, Republic of Korea in 2011, and her PhD in Chemistry from Pohang University of Science and Technology, Pohang,

Republic of Korea in 2016. She is currently a researcher at the Electronics and Telecommunications Research Institute, Daejeon, Republic of Korea. Her

current research interests are optoelectronic devices with quantum dots (QDs) and organics, such as QLEDs and OLEDs.



Jin-Wook Shin received his BS and MS degrees from Myongji University and Kwangwoon University, Republic of Korea, respectively. In 2018, he received his PhD degree from Tohoku University, Japan. He joined Electronics and Telecommunications

Research Institute, Daejeon, Republic of Korea in 2009. His current research interests include flexible display devices, microdisplays for augmented reality/virtual reality, and implantable biomedical devices.

SUPPORTING INFORMATION

Additional supporting information can be found online in the Supporting Information section at the end of this article.

How to cite this article: H. Cho, C. W. Joo, B.-H. Kwon, C. Kang, S. Choi, and J. W. Sin, *Correlation between optimized thicknesses of capping layer and thin metal electrode for efficient top-emitting blue organic light-emitting diodes*, ETRI Journal **45** (2023), 1056–1064. DOI [10.4218/etrij.2022-0236](https://doi.org/10.4218/etrij.2022-0236)